DOI: 10.1021/ic902571q

Inorganic Chemistry
Article

Structure, Photophysical Properties, and DFT Calculations of Selenide-Centered Pentacapped Trigonal Prismatic Silver(I) Clusters

C. W. Liu,*,† Ching-Shiang Feng,† Rei-Jen Fu,† Hao-Wei Chang,† Jean-Yves Saillard,*,‡ Samia Kahlal,‡ Ju-Chun Wang,§ and I-Jy Chang⊥

†*Department of Chemistry, National Dong Hwa University, Hualien, Taiwan 97401, Republic of China,* ‡*UMR-CNRS, 6226 "Sciences Chimiques de Rennes", Université de Rennes 1, 35042 Rennes Cedex, France,* §*Department of Chemistry, Soochow University, Taipei, Taiwan 111, Republic of China, and* ⊥*Department of Chemistry, National Taiwan Normal University, Taipei, Taiwan 114, Republic of China*

Received December 24, 2009

Undecanuclear silver clusters $[Ag_{11}(\mu_9\text{-Se})(\mu_3\text{-Br})_3\{Se_2P(OR)_2\}_6]$ (R = Et, ^{i}Pr, ^{2}Bu) were isolated from the reaction of $[Ag(CH_3CN)_4](PF_6)$, $NH_4[Se_2P(OR)_2]$, and Bu_4NBr in a molar ratio of 4:3:1 in CH_2Cl_2 at −20 °C. Clusters were characterized by elemental analysis, NMR spectroscopy (^{1}H, ^{31}P, and ^{77}Se), positive FAB mass spectrometry, and X-ray crystallography of the isopropyl derivative. Structural elucidations revealed that the $Ag_{11}Se$ core geometry of clusters is a selenide-centered, slightly distorted 3,3,4,4,4-pentacapped trigonal prism surrounded by six diselenophosphato ligands, each in a tetrametallic tetraconnective (μ_2, μ_2) coordination mode, and three μ_3-bromide anions. All compounds exhibited orange luminescence both as a solid and in solution. The electronic structure of these clusters was studied by DFT calculations, and their optical properties were rationalized through a TDDFT investigation. The computed metrical parameters of the clusters were consistent with the corresponding X-ray data of $[Ag_{11}(\mu_9\text{-Se})(\mu_3\text{-Br})_3\{Se_2P(O^iPr)_2\}_6]$. The theoretical investigations affirmed that the low-energy absorptions as well as emissions were due to transitions from an orbital mostly of a selenophosphate ligand/central Se atom character to an orbital of metal character.

Introduction

Clusters form a type of material that is intermediate between single atoms and bulk matter.[1] Coinage metal clusters are particularly enthralling, as they appear to involve the remarkable versatility of the metal's coordination environment and geometry.[2] The chemistry of clusters that contain an encapsulated main-group element is fascinating when one considers their intriguing electronic and luminescent properties, which have potential applications in various optical and sensing devices.[3] While the chemistry of halide-encapsulated clusters has received considerable attention[4] and has been the subject of many studies, corresponding chalcogenide-encapsulated clusters or cages remain comparatively less well explored. However, a small number of sulfur-encapsulated clusters are known.[5] Selenium-encapsulated compounds have received attention only in recent years since we prepared and reported the first selenide-centered cubic copper and silver clusters with diselenophosphate (dsep) ligands.[6] We subsequently focused our attention on the synthesis of molecular clusters containing an interstitial main-group element with diverse geometries. In the course of these efforts, and through the use of various combinations of metal precursors, ligands, and interstitial ions, a large number of clusters have been synthesized with different molar ratios of metal precursors

*To whom correspondence should be addressed. E-mail: chenwei@mail.ndhu.edu.tw.

(1) Castleman, A. W.; Khanna, S. N. *J. Phys. Chem. C* **2009**, *113*, 2664–2675.

(2) (a) Su, W.; Hong, M. *Angew. Chem., Int. Ed.* **2000**, *39*, 2911–2914. (b) Shimizu, G. K. H; Enright, G. D. *Chem. Commun.* **1999**, 1485–1486. (c) John, F. C.; Fenske, D.; Power, W. P. *Angew. Chem., Int. Ed. Engl.* **1997**, *36*, 1176–1179. (d) Eduardo, J. F.; Concepción, G. M.; Laguna, A. *J. Am. Chem. Soc.* **2000**, *122*, 7287–7293. (e) Youngme, S.; Phuengphai, P.; Chaichit, N. *Inorg. Chim. Acta* **2005**, *358*, 849–853.

(3) Chen, W.; Wang, Z.; Lin, L. *Phys. Lett. A* **1997**, *232*, 391–394.

(4) (a) Wang, R.; Selby, H. D.; Liu, H.; Carducci, M. D.; Jin, T.; Zhang, Z.; Anthis, J. W.; Staples, R. J. *Inorg. Chem.* **2002**, *41*, 278–286. (b) Wang, R.; Jin, T.; Zhang, Z.; Staples, R. J. *Angew. Chem., Int. Ed.* **1999**, *38*, 1813–1815. (c) Yang, X.; Knobler, C. B.; Hawthorne, M. F. *Angew. Chem., Int. Ed. Engl.* **1991**, *11*, 1507–1508. (d) Gonzalez-Duarte, P.; Clegg, W.; Casals, I.; Sola, J.; Rius, J. *J. Am. Chem. Soc.* **1998**, *120*, 1260–1266. (e) Dance, I. G. *Aust. J. Chem.* **1985**, *38*, 1391–1394. (f) Krautscheid, H.; Lode, C.; Vielsack, F.; Vollmer, H. *J. Chem. Soc., Dalton Trans.* **2001**, 1099–1104. (g) Lee, H.; Knobler, C. B.; Hawthorne, M. F. *Angew. Chem., Int. Ed.* **2000**, *39*, 776–778. (h) Wang, Q.-M.; Mak, T. C. W. *Chem. Commun.* **2000**, 1435–1436.

(5) (a) Liu, C. W.; Stubbs, R. T.; Staples, R. J.; Fackler, J. P., Jr. *J. Am. Chem. Soc.* **1995**, *117*, 9778–9779. (b) Adams, R. D.; Wolfe, T. A.; Wu, W. *Polyhedron* **1991**, *10*, 447–454. (c) Matsumoto, K.; Tanaka, R.; Shimomura, R.; Nakao, Y. *Inorg. Chim. Acta* **2000**, *304*, 293–296.

(6) (a) Liu, C. W.; Chen, H.-C.; Wang, J.-C.; Keng, T.-C. *Chem. Commun.* **1998**, 1831–1832. (b) Liu, C. W.; Shang, I.-J.; Wang, J.-C.; Keng, T.-J. *Chem. Commun.* **1999**, 995–996.

Published on Web 05/11/2010

and ligands, and thus simple synthetic routes for the main-group element-encapsulated clusters have been unambiguously established. Recently, we have reported some nonacoordinated selenide-encapsulated Ag_{11} clusters, $Ag_{11}(\mu_9\text{-Se})(\mu_3\text{-I})_3[Se_2P(OR)_2]_6$, in which 11 silver atoms adopt a pentacapped trigonal-prismatic geometry.[7] Clusters or cages with the geometry of a pentacapped trigonal prism are not common,[8] and the isolated undecanuclear silver clusters are a remarkable example of a 3,3,4,4,4-pentacapped trigonal-prisimatic silver framework. Commonly, most luminescent Ag(I) compounds exhibit emission at low temperatures,[9] and few Ag(I) compounds are known to be luminescent at room temperature.[10] However, our Ag_{11} clusters are a notable example of compounds with photoluminescent properties at both ambient and cryogenic temperatures in solution as well as in the solid state. Hence, as part of our enduring interest in main-group element-encapsulated cluster synthesis, we extended our efforts to synthesizing a new set of selenide-encapsulated silver clusters containing a hub of 11 silver atoms with pentacapped trigonal-prism geometry. Herein, we report the detailed synthesis and characterization of undecanuclear silver clusters $[Ag_{11}(\mu_9\text{-Se})(\mu_3\text{-Br})_3\{Se_2P(OR)_2\}_6]$ (R = Et, **1**; ^{i}Pr, **2**; ^{2}Bu, **3**). In addition, we studied the electronic structure of these clusters by DFT calculations and rationalized their optical properties through a TDDFT investigation. Similar to their iodide analogues, the present clusters also exhibited luminescent properties at room temperature as well as at low temperatures both in solution and in the solid state.

Experimental Section

All chemicals were of analytical grade available commercially and were used as received. Solvents were purified following standard procedures.[11] Standard Schlenk techniques were employed for performing all reactions under an inert atmosphere. The starting silver(I) complexes, $Ag(CH_3CN)_4(PF_6)$[12] and $[Ag_{10}(Se)\{Se_2P(OR)_2\}_8]$,[13] and the ligands, $NH_4Se_2P(OR)_2$ (R = Et, ^{i}Pr, ^{2}Bu),[14] were prepared according to the literature methods. The elemental analyses were done using a Perkin-Elmer 2400 CHN analyzer. ^{1}H, ^{31}P, and ^{77}Se NMR spectra were recorded on an Advance-300 Fourier transform spectrometer. H_3PO_4 ($\delta = 0$) and PhSeSePh ($\delta = 463$) were used as the external reference for ^{31}P and ^{77}Se NMR, respectively. Positive fast atom bombardment (FAB) mass spectra were carried out on a VG 70-250S mass spectrometer with nitrobenzyl alcohol as the matrix. UV−visible absorption spectra were recorded on a HP 8453 photodiode array spectrometer. Emission spectra were recorded on a Cary Eclipse B10 fluorescence spectrophotometer. Emission spectra were corrected for instrumental responses. Integrated emission quantum yields, Φ_{em}, were estimated relative to that of $Ru(bipy)_3^{2+}$ ($\Phi_{em} = 0.06$) as a reference. Excited-state lifetimes were measured by a home-constructed, time-resolved laser spectrometer. The instrument was equipped with a Quanta Ray GCR-170 pulsed Nd:YAG laser. The third harmonic (355 nm, fwhm = 10 ns) was used as an excitation source. Emission signals were focused into an ARC SpectraPro-500 double monochromator. The monochromator output was sent into a photomultiplier tube (Hamamatsu R928). The signal was further amplified by a homemade fast amplifier before being sent into a digitizer (LeCory 9350A). Decay traces were transferred to a personal computer loaded with the commercial software Origin 3.5. All experimental data were fitted by a single-exponential decay.

Preparation of $[Ag_{11}(\mu_9\text{-Se})(\mu_3\text{-Br})_3\{Se_2P(OR)_2\}_6]$ (R = Et, 1; ^{i}Pr, 2; ^{2}Bu, 3). Compounds **1**−**3** can be prepared by following a general procedure; nevertheless clusters **1** and **2** can also be prepared in a comparatively high yield by employing another preparative method. A detailed procedure for **2** is given below.

Method a (1−3). A solution of $NH_4Se_2P(OC_3H_7)_2$ (0.58 g, 1.78 mmol) and $^nBu_4NBr$ (0.19 g, 0.60 mmol) in 30 mL of CH_2Cl_2 was stirred at −20 °C for 30 min. To this solution was added $[Ag(CH_3CN)_4PF_6]$ (0.992 g, 2.38 mmol), and the mixture was stirred for 12 h at −20 °C under a dinitrogen atmosphere. After filtration, the filtrate was washed with deionized water to afford a yellow solution. The residue obtained after evaporating the solvent was washed with hexanes and dissolved in diethyl ether. Yellow products obtained after drying were recrystallized from CH_2Cl_2/hexanes. Yield: 46%. Anal. Calcd for $C_{36}H_{84}Ag_{11}O_{12}P_6Se_{13}Br_3$: C, 12.92; H, 2.53. Found: C, 12.35; H, 2.35. FAB-MS: m/z 3267.3 $(M - Br)^+$, 3040.57 $(M - dsep)^+$. ^{1}H NMR (300 MHz, $CDCl_3$): δ 1.38 [d, 72H, CH_3, $^3J_{HH} = 7$ Hz], 4.78 [m, 6H, CH], 5.17 [m, 6H, CH]. ^{31}P{^{1}H} NMR (121 MHz, $CDCl_3$): δ 77.4 [s, 6P, $J_{PSe} = 657$ Hz]. ^{77}Se{^{1}H} NMR (57 MHz, $CDCl_3$): δ 54.9 (d, $J_{SeP} = 678$ Hz, 6Se), 58.9 (d, $J_{SeP} = 653$ Hz, 6Se), −1257 (s, 1Se).

Method b (1 and 2). $Ag_{10}(Se)[Se_2P(OEt)_2]_8$ (150 mg, 0.044 mmol) and $Ag(CH_3CN)_4PF_6$ (19 mg, 0.045 mmol) in CH_2Cl_2 (30 mL) at −20 °C were stirred for 1 h; then $^nBu_4NBr$ (43 mg, 0.133 mmol) was added. The solution mixture was stirred for 15 h at −20 °C under a dinitrogen atmosphere. After filtration, the filtrate was washed with deionized water (150 mL) several times to afford a yellow solution. Then the solvent was evaporated under vacuum, and the residue was washed with hexanes. This was collected by filtration, redissolved in diethyl ether, and dried under vacuum to obtain a yellow powder. Yield: 51.7%.

Compound 1. Yield: 45%, 0.785 g. Anal. Calcd for $C_{24}H_{60}Ag_{11}O_{12}P_6Se_{13}Br_3 \cdot C_6H_{14}$: C, 11.03; H, 2.28. Found: C, 10.98; H, 2.35. FAB-MS: m/z 3099.3 $(M - Br)^+$, 2900.37 $(M - dsep)^+$. ^{1}H NMR (300 MHz, $CDCl_3$): δ 1.37 [t, 36H, CH_3, $^3J_{HH} = 7$ Hz], 4.16 [m, 12H, CH_2], 4.34 [m, 12H, CH_2]. ^{31}P{^{1}H} NMR (121 MHz, $CDCl_3$): δ 83.1 [s, 6P, $J_{PSe} = 664$ Hz]. ^{77}Se{^{1}H} NMR (57 MHz, $CDCl_3$): δ 29.2 (d, $J_{SeP} = 671$ Hz, 6Se), 36.3 (d, $J_{SeP} = 660$ Hz, 6Se), −1236 (s, 1Se).

Compound 3. Yield: 60.7%. Anal. Calcd for $C_{48}H_{108}Ag_{11}O_{12}P_6Se_{13}Br_3 \cdot 1/2C_6H_{14}$: C, 17.21; H, 3.26. Found: C, 16.98; H, 3.01. FAB-MS: m/z 3436.1 $(M - Br)^+$, 3179.8 $(M - dsep)^+$. ^{1}H NMR (300 MHz, $CDCl_3$): δ 0.94 (t, 36H, OCH(CH_3)CH_2CH_3), 1.38 (d, 36H, OCH(CH_3)CH_2CH_3), 1.67 (m, 24H, OCH(CH_3)CH_2CH_3), 4.57 (m, 6H, OCH(CH_3)CH_2CH_3), 5.00 (m, 6H, OCH(CH_3)CH_2CH_3). ^{31}P{^{1}H} NMR (121 MHz, $CDCl_3$): δ 77.5 [s, 6P, $J_{P-Se} = 663$ Hz]. ^{77}Se{^{1}H} NMR (57 MHz, $CDCl_3$): δ 67.5 (d, $J_{SeP} = 642$ Hz, 6Se), 70.7 (d, $J_{SeP} = 677$ Hz, 6Se), −1256 (s, 1Se).

(7) Liu, C. W.; Shang, L. J.; Fu, R. -J.; Wang, J.-C.; Chang, I.-J. *Inorg. Chem.* **2006**, *45*, 2335–2340.

(8) (a) Fenske, D.; Ohmer, J. *Angew. Chem., Int. Ed. Engl.* **1987**, *26*, 148–151. (b) Mahdjour-Hassan-Abadi, F.; Hartl, H.; Fuchs, J. *Angew. Chem., Int. Ed. Engl.* **1984**, *23*, 514–515. (c) Huang, Z. Y.; Lei, X. J.; Hong, M. C.; Liu, H. Q. *Inorg. Chem.* **1992**, *31*, 2990–2991.

(9) (a) Yam, V. W. W.; Lo, K. K.-W. W.; Fung, K.-M. *Coord. Chem. Rev.* **1998**, *171*, 17–41. (b) Harvey, P. D; Fortin, D. *Coord. Chem. Rev.* **1998**, *171*, 351–354. (c) Omary, M. A; Patterson, H. H. *J. Am. Chem. Soc.* **1998**, *120*, 7696–7705.

(10) (a) Tong, M.-L; Chen, X.-M; Ye, B.-H. *Angew. Chem., Int. Ed.* **1999**, *38*, 2237–2240. (b) Tong, M.-L.; Yu, X.-L; Chen, X.-M. *Inorg. Chem. Commun.* **2000**, *3*, 694–696. (c) Zheng, S.-L; Tong, M.-L; Tan, S.-D. *Organometallics* **2001**, *20*, 5319–5325. (d) Yam, V. W. W.; Lo, K. K.-W.; Wang, C. R.; Cheung, K. K. *Inorg. Chem.* **1996**, *35*, 5116–5117. (e) Catalano, V. J.; Kar, H. M.; Garnas, J. *Angew. Chem., Int. Ed.* **1999**, *38*, 1979–1982.

(11) Perrin, D. D.; Armarego, W. L. F.; Perrin, D. R. *Purification of Laboratory Chemicals*, 2nd ed.; Pergamon Press: Oxford, 1980.

(12) Nelsson, K.; Oskarsson, A. *Acta Chem. Scand., Sect. A* **1984**, *38*, 79–81.

(13) Liu, C. W.; Hung, C.-M.; Wang, J.-C.; Keng, T.-C. *J. Chem. Soc., Dalton. Trans.* **2002**, 3482–3488.

(14) Sarkar, B.; Fang, C.-S.; Yu, L.-Y.; Wang, J.-C.; Liu, C. W. *New J. Chem.* **2009**, *33*, 626–633.

Table 1. Selected Crystallographic Data for **2**

chemical formula	$C_{36}H_{84}Ag_{11}Br_3O_{12}P_6Se_{13}$
fw	3347.63
cryst syst	monoclinic
space group	$P2(1)/n$
a (Å)	14.7044 (11)
b (Å)	22.9372 (17)
c (Å)	24.7295 (19)
β (deg)	91.928 (2)
V (Å^3)	8336.0 (11)
Z	4
ρ_{calc} (mg/m^3)	2.667
μ (mm^{-1})	9.794
reflns collected	72 876
unique reflns	14 807 [R_{int} = 0.0451]
reflns ($I \geq 2\sigma(I)$)	8789
params	652
GOF on F^2	1.050
R_1,[a] wR_2[b] ($I \geq 2\sigma(I)$)	0.0601, 0.1458
largest peak and hole (e/Å^3)	1.571, −1.627

[a] $R_1 = \sum||F_o| - |F_c||/\sum|F_o|$. [b] $wR_2 = \{\sum[w(F_o^2 - F_c^2)^2]/\sum[w(F_o^2)^2]\}^{1/2}$.

X-ray Crystallography. Crystallographic data of $Ag_{11}(\mu_9\text{-Se})(\mu_3\text{-Br})_3[Se_2P(O^iPr)_2]_6$ (**2**) are given in Table 1. Yellow crystals of **2** were obtained by diffusion of a dichloromethane solution of the cluster into a layer of hexanes. Suitable single crystals of compounds **1** and **3** could not be obtained for data collection despite repeated efforts. Intensity data of **2** were collected at 223 K on a Bruker APEX-II CCD diffractometer. The unit cell parameters were calculated and refined from the full data set. The SMART software[15] was used for data acquisition, and the SAINT-Plus[16] software was used for data reduction. The absorption corrections were performed with the help of the SADABS[17] program. The structure was solved by direct methods and refined by full-matrix least-squares on F^2 using the SHELXTL software package incorporated in SHELXTL/PC version 5.10.[18] Three oxygen atoms were disordered over two sites, each in 50% occupancy, and refined isotropically. Fifteen carbon atoms of the dsep ligands were refined isotropically with fixed thermal parameters and distance constraints. All other nonhydrogen atoms were refined anisotropically. H atoms were added in the idealized position except three methine protons. The asymmetric unit comprised one cluster molecule, and the bond parameters of interest are listed in Table 2.

Computational Details. Ab initio calculations were carried out using the Gaussian 03 package,[19] employing PBE1PBE (PBE0) functionals[20] and using a standard double-ξ polarized basis set, namely, the LANL2DZ set, augmented with Ahlrichs polarization functions on all the atoms. The optimized geometries were fully characterized as true minima via analytical frequency calculations (no imaginary eigenvalues). The geometries obtained from DFT calculations were used to perform NBO analysis with the NBO 5.0 program.[21] The composition of the molecular orbitals was calculated using the AOMix program.[22] The UV−visible transitions were calculated by means of time-dependent DFT (TDDFT) calculations,[23] at the same level of theory. Only singlet−singlet transitions, that is, spin-allowed transitions, have been taken into account. Moreover, only transitions with non-negligible oscillator strengths are reported and discussed. Representation of the molecular structures was done using the program MOLEKEL 4.3.[24] The UV−visible spectra were simulated from the computed TDDFT transitions and their oscillator strengths by using the SWizard program,[25] each transition being associated with a Gaussian function of half-height width equal to 3000 cm^{-1}.

Results and Discussion

Synthesis and Characterization. We have previously reported an efficient synthesis for undecanuclear silver clusters, $Ag_{11}(\mu_9\text{-Se})(\mu_3\text{-I})_3[Se_2P(OR)_2]_6$.[7] This method was used for the preparation of their analogous $[Ag_{11}(\mu_9\text{-Se})(\mu_3\text{-Br})_3\{Se_2P(OR)_2\}_6]$ clusters. The formation of clusters **1**−**3** is illustrated in Scheme 1. The clusters $[Ag_{11}(\mu_9\text{-Se})(\mu_3\text{-Br})_3\{Se_2P(OEt)_2\}_6]$ (**1**), $[Ag_{11}(\mu_9\text{-Se})(\mu_3\text{-Br})_3\{Se_2P(O^iPr)_2\}_6]$ (**2**), and $[Ag_{11}(\mu_9\text{-Se})(\mu_3\text{-Br})_3\{Se_2P(O^2Bu)_2\}_6]$ (**3**) were synthesized in 45−61% yield from the reaction of $Ag(CH_3CN)_4PF_6$, $NH_4Se_2P(OR)_2$, and Bu_4NBr in a molar ratio of 4:3:1 in dichloromethane at −20 °C. Clusters **1** and **2** were also isolated in comparatively higher yield (51−67%) from the reaction of $[Ag_{10}(Se)\{Se_2P(OR)_2\}_8]$ (R = Et, ^{i}Pr), $[Ag(CH_3CN)_4](PF_6)$, and Bu_4NBr in a 1:1:3 molar ratio at ambient temperature (Scheme 1), but the unavailability of $[Ag_{10}(Se)\{Se_2P(O^2Bu)_2\}_8]$ precluded the preparation of **3** from the Ag_{10} cluster. Nevertheless, when the reaction was carried out at 0 °C, bromide-centered Ag_8 clusters were isolated as the major product together with a small quantity of selenium-centered Ag_{10} clusters, and selenium-centered Ag_{11} clusters were not formed.[26] This result was not surprising, as the halide-centered cubic clusters were the major product under identical experimental conditions in our previous work.[27] Compounds **1**−**3** were characterized by elemental analysis, FAB-MS, multinuclear NMR (^{1}H, ^{31}P, ^{77}Se), and X-ray diffraction techniques. The elemental analysis data of the clusters were consistent with the molecular formula of **1**−**3**. The positive FAB mass spectra of the three clusters were comprised of two bands corresponding to $[Ag_{11}(\mu_9\text{-Se})(\mu_3\text{-Br})_2\{Se_2P(OR)_2\}_6]^+$ and $[Ag_{11}(\mu_9\text{-Se})(\mu_3\text{-Br})_3\{Se_2P(OR)_2\}_5]^+$ moieties, which formed after the loss of one bromide ion and one dsep ligand, respectively, from the parent clusters, similar to that of the isostructural undecanuclear copper clusters.[28] This provides further evidence for the composition of **1**−**3**. The formation of clusters according to Scheme 1 was followed

(15) *SMART V4.043*: Software for the CCD Detector System; Bruker Analytical X-ray System: Madison, WI, **1995**.
(16) *SAINT V4.043*: Software for the CCD Detector System; Bruker Analytical X-ray System: Madison, WI, **1995**.
(17) Sheldrick, G. M. *SADABS*; University of Gottingen: Gottingen, Germany, **1996**.
(18) *SHELXL 5.10* (PC Version): Program Library for Structure Solution and Molecular Graphics; Bruker Analytical X-ray System: Madison, WI, 1997.
(19) Frisch, M. J.; et al. et al. *Gaussian 03*, Revision B.04; Gaussian, Inc.: Pittsburgh, PA, 2003. A full reference for Gaussian programs is provided in the Supporting Information.
(20) (a) Perdew, J. P.; Ernzerhof; Burke, K. M. *J. Chem. Phys.* **1996**, *105*, 9982–9985. (b) Perdew, J. P.; Burke, K.; Ernzerhof, M. *Phys. Rev. Lett.* **1996**, *77*, 3865–3868. (c) Perdew, J. P.; Burke, K.; Ernzerhof, M. *Phys. Rev. Lett.* **1997**, *78*, 1396–1396.
(21) Glendening, E. D.; Badenhoop, J. K.; Reed, A. E.; Carpenter, J. E.; Bohmann, J. A.; Morales, C. M.; Weinhold, F. *NBO 5.0*; Theoretical Chemistry Institute, University of Wisconsin, Madison, WI, 2001, http://www.chem.wisc.edu/~nbo5.
(22) Gorelsky, S. I. *AOMix* program, http://www.sg-chem.net/.
(23) Burke, K.; Gross, E. K. U. A guided tour of time-dependent density functional theory. In *Density Functionals: Theory and Applications*, Lecture Notes in Physics, Vol. *500*; Joubert, D., Ed.; Springer, 1998.
(24) Flukiger, P.; Luthi, H. P.; Portmann, S.; Weber, J. *MOLEKEL 4.3*; Swiss Center for Scientific Computing: Manno, Switzerland, 2000, http://www.cscs.ch/.
(25) Gorelsky, S. I. *SWizard* program, revision 4.5, http://www.sg-chem.net/.
(26) Liu, C. W.; Haia, H.-C.; Hung, C.-M.; Santra, B. K.; Liaw, B.-J.; Lin, Z.; Wang, J.-C. *Inorg. Chem.* **2004**, *43*, 4464–4470.
(27) Liu, C. W.; Hung, C.-M.; Santra, B. K.; Chen, H.-C.; Hsueh, H.-H.; Wang, J.-C. *Inorg. Chem.* **2003**, *42*, 3216–3220.
(28) Liu, C. W.; Hung, C.-M.; Santra, B. K.; Chu, Y.-H.; Wang, J.-C.; Lin, Z. *Inorg. Chem.* **2004**, *43*, 4306–4316.

Table 2. Selected Bond Distances (Å) and Angles (deg) of **2**

Ag_1-Ag_3	3.1324 (17)	Ag_5-Se_8	2.5837 (18)	$Ag_3-Br_2-Ag_1$	70.80 (5)
Ag_1-Ag_8	3.3089 (18)	Ag_5-Se_{10}	2.5872 (18)	$Ag_3-Br_2-Ag_8$	69.61 (5)
Ag_1-Ag_{10}	3.1061 (18)	Ag_6-Se_9	2.6513 (18)	$Ag_1-Br_2-Ag_8$	73.35 (5)
Ag_2-Ag_3	3.2881 (18)	Ag_6-Se_{11}	2.6150 (17)	$Ag_{11}-Br_3-Ag_2$	71.05 (5)
Ag_2-Ag_4	3.3467 (19)	Ag_7-Se_7	2.6318 (19)	$Ag_{11}-Br_3-Ag_4$	69.69 (5)
Ag_2-Ag_{10}	3.0840 (18)	Ag_7-Se_{10}	2.6327 (19)	$Ag_2-Br_3-Ag_4$	73.65 (5)
Ag_2-Ag_{11}	3.1606 (18)	Ag_8-Se_4	2.634 (2)		
Ag_3-Ag_4	3.3359 (19)	Ag_8-Se_9	2.650 (2)		
Ag_3-Ag_8	3.0939 (18)	Ag_9-Se_{12}	2.6625 (19)		
Ag_4-Ag_5	3.0448 (18)	$Ag_{10}-Se_{12}$	2.5745 (19)		
Ag_4-Ag_{11}	3.122 (2)	$Ag_{10}-Se_6$	2.5842 (18)		
Ag_5-Ag_8	3.0728 (18)	$Ag_{10}-Se_2$	2.5897 (19)		
Ag_5-Ag_7	3.0922 (19)	$Ag_{11}-Se_7$	2.619 (2)		
Ag_6-Ag_7	3.0497 (16)	$Ag_{11}-Se_5$	2.627 (2)		
Ag_6-Ag_9	3.1226 (18)	Ag_1-Br_2	2.7640 (19)		
Ag_7-Ag_9	3.3498 (18)	Ag_3-Br_2	2.6408 (19)		
Ag_9-Ag_{10}	3.0422 (18)	Ag_8-Br_2	2.776 (2)		
Ag_9-Ag_{11}	3.3164 (19)	Ag_6-Br_1	2.6248 (18)		
Ag_1-Se_{13}	2.783 (2)	Ag_7-Br_1	2.782 (2)		
Ag_2-Se_{13}	2.776 (2)	Ag_9-Br_1	2.781 (2)		
Ag_4-Se_{13}	2.731 (2)	Ag_2-Br_3	2.7802 (19)		
Ag_6-Se_{13}	3.0879 (19)	Ag_4-Br_3	2.803 (2)		
Ag_7-Se_{13}	2.800 (2)	$Ag_{11}-Br_3$	2.656 (2)		
Ag_8-Se_{13}	2.796 (2)				
Ag_9-Se_{13}	2.778 (2)	$Ag_8-Se_{13}-Ag_7$	87.98 (6)		
Ag_1-Se_2	2.6233 (19)	$Ag_4-Se_{13}-Ag_6$	140.68 (7)		
Ag_1-Se_{11}	2.6516 (19)	$Ag_2-Se_{13}-Ag_6$	144.16 (7)		
Ag_2-Se_1	2.655 (2)	$Ag_9-Se_{13}-Ag_6$	64.07 (5)		
Ag_2-Se_6	2.649 (2)	$Ag_1-Se_{13}-Ag_6$	70.89 (5)		
Ag_3-Se_1	2.594 (2)	$Ag_8-Se_{13}-Ag_6$	71.46 (5)		
Ag_3-Se_3	2.6305 (19)	$Ag_7-Se_{13}-Ag_6$	62.16 (4)		
Ag_4-Se_3	2.667 (2)	$Ag_6-Br_1-Ag_9$	70.50 (5)		
Ag_4-Se_8	2.647 (2)	$Ag_6-Br_1-Ag_7$	68.60 (5)		
Ag_5-Se_4	2.584 (2)	$Ag_9-Br_1-Ag_7$	74.05 (6)		

Scheme 1

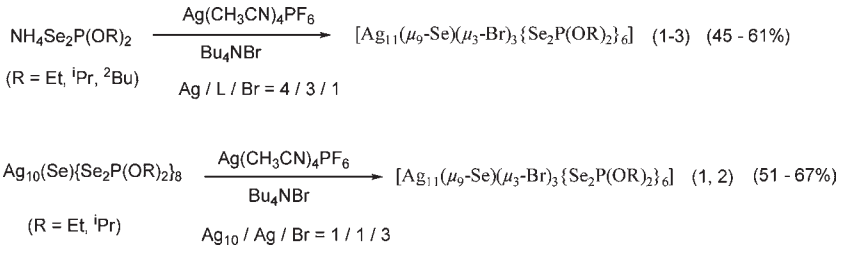

by ^{31}P NMR spectroscopy. Unlike the analogous undecanuclear copper clusters, the ^{31}P NMR spectra of compounds **1**−**3** at ambient temperature featured a singlet at δ 83.1, 77.4, and 77.5 ppm, respectively, with one set of satellites (667.0, 658.9, and 655.2 Hz, respectively) due to P−Se coupling. The presence of only one set of Se satellites could be due to the poor spectral resolution. Nevertheless, the inequivalence of Se nuclei in the dsep ligand was supported by two sets of doublets observed in the $^{77}Se\{^1H\}$ NMR spectrum (δ 29.2 ppm, J_{Se-P} 671 Hz, and δ 36.3 ppm, J_{Se-P} 660 Hz of **1**). In addition the presence of two chemical shifts for the methylene protons in the ^1H NMR spectrum of **1** clearly suggests the lack of a 2-fold rotational axis imposed on the dsep ligand (*vide infra*). The ^{77}Se NMR spectra of **2** and **3** display a similar pattern to that observed in **1** (see Experimental Section). Finally the central selenium atom of **1**−**3** is detected unequivocally by ^{77}Se NMR with a resonance frequency at −1236, −1257, and −1256 ppm, respectively. These chemical shifts lie in the same range as their copper analogues.[28] Overall the NMR data suggest that all six dsep ligands are equivalent in solution. Attempts to isolate the corresponding chloro complexes were not successful; instead only chloride-centered Ag_8 cubic clusters were formed.

Structure of $Ag_{11}(\mu_9\text{-Se})(\mu_3\text{-Br})_3[Se_2P(O^iPr)_2]_6$ (2). Figure 1 shows the molecular structure of $Ag_{11}(\mu_9\text{-Se})(\mu_3\text{-Br})_3[Se_2P(O^iPr)_2]_6$ (**2**), the structure being isomorphous to that of its iodide analogue $Ag_{11}(\mu_9\text{-Se})(\mu_3\text{-I})_3[Se_2P(O^iPr)_2]_6$.[7] The cluster is crystallized in the monoclinic space group $P2_1/n$ with one molecule in the asymmetric unit. Bond distances and angles of interest in **2** are given in Table 2. The cluster features a three-dimensional framework comprising a hub of 11 silver atoms with the geometry of a slightly distorted 3,3,4,4,4-pentacapped trigonal prism containing an encapsulated selenium atom with a 9-fold coordination mode, and the exterior of the central pentacapped-trigonal prism is further bridged by three bromide and six dsep ligands. In the cluster molecule six silver atoms, Ag1, Ag2, Ag4, Ag7, Ag8, and Ag9, the six vertexes, generate a trigonal prism, and the three rectangular and two triangular faces of the resulting trigonal prism are further capped by additional silver atoms. The $Ag_{11}Se$ core exhibits a D_{3h} symmetry with a pseudo-3-fold axis that passes through the Ag5, Se13, and

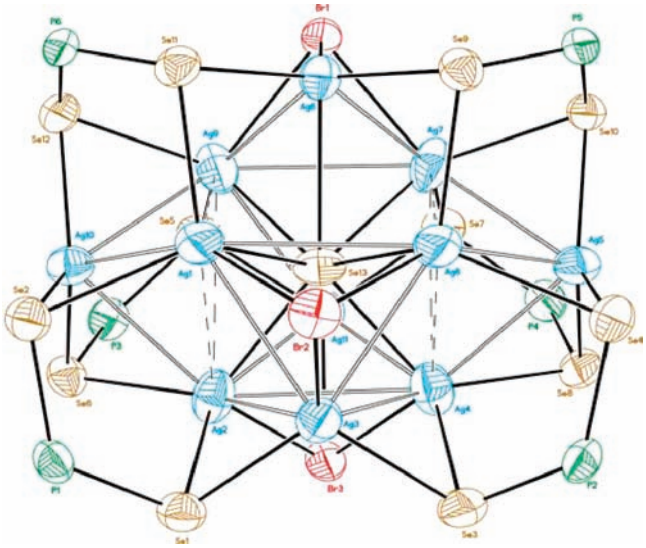

Figure 1. Thermal ellipsoid drawing of **2** with isopropoxy groups omitted for clarity.

Ag10 atoms. A clear view of the $Ag_{11}Se$ core unit of the cluster is shown in Figure 2. With the exception of our earlier studies,[7,13,28] few reports are available on clusters containing 11 core metal atoms with a pentacapped trigonal-prismatic geometry.[29] The cluster exhibits a longer Ag−Ag distance in the range 3.741(20)−3.941(20) Å along the edges of the trigonal prism and a shorter bond with an average of 3.335(20) Å between Ag1−Ag8, Ag7−Ag9, and Ag2−Ag4. The structural pattern of the cluster can also be described as a coalition of nine Ag_4 butterflies, where the wing-tip positions are represented by five capping silver atoms, with each edge of the trigonal prism being a hinge. The central selenium atom is bound to nine metal atoms, and there are two sets of bond lengths. Among these, one set of three bond lengths is relatively longer (Ag3−Se13, Ag6−Se13, and Ag11−Se13, at 3.146, 3.086, and 3.118 Å, respectively) than that of the other set of six bond lengths. These bond lengths are comparable to the $Ag-Se_{center}$ bond lengths of the iodide analogue and are much shorter than the sum of their van der Waals radii of 3.72 Å.[30] The other set of $Ag-Se_{center}$ bond lengths were consistent with those observed in related systems.[31] The $Ag-Se_{center}-Ag$ angles of the cluster were in the range 62.16(4)−144.16(7)°. The key feature of the cluster, i.e., the $Ag_{11}Se$ hub, is further stabilized by three bromides and six dsep ligands. The dsep ligands in **2** adopt a tetrametallic tetraconnective (μ_2, μ_2) bridging mode,[32] with each Se atom bridging two Ag atoms, one located at the vertex and the other at the capping site. In other words, the six Ag_4 butterflies containing a silver atom on the C_3 axis are each capped by a dsep ligand in a μ_2, μ_2 coordination pattern. The Ag−μ_2-Se bond distance is in

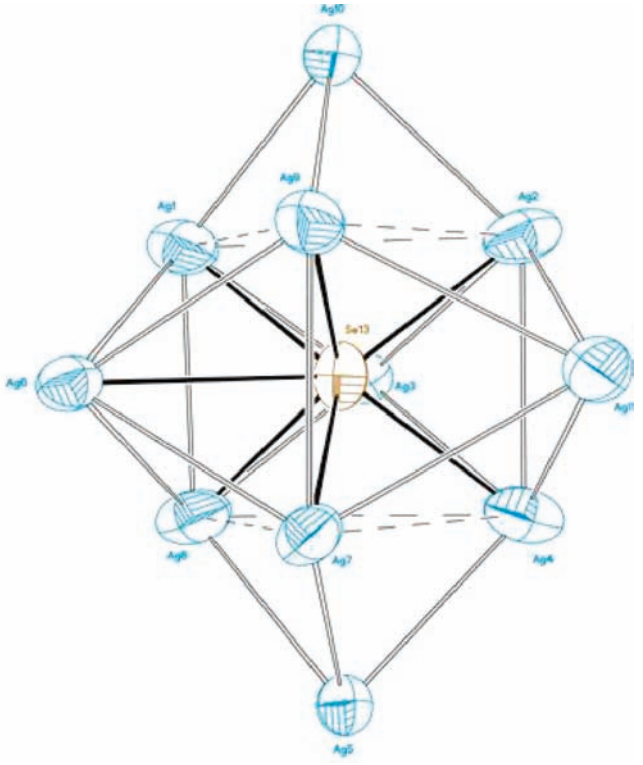

Figure 2. $Ag_{11}Se$ core unit of cluster **2**.

the range 2.584(2)−2.667(2) Å and the Ag−μ_2Se−Ag angles range between 71.01(6)° and 81.31(6)°. The P−Se distances are an average of 2.155(5) Å. The remaining three Ag_4 butterflies, where the hinge positions are the sides of the prism, are capped by a triply bridging bromide atom over an alternating set of three of the six triangular faces. The average Ag−Br bond distance is 2.734(2) Å. The Ag−Br−Ag angles are in the range 68.60(5)−74.05(6)°. Thus out of the total of 11 silver atoms, two atoms, which are located on the C_3 axis, are trigonally coordinated by three selenium atoms, and the rest are tetragonally coordinated by three selenium atoms, two from desp ligands and one central selenide, and one from a bromine atom. Hence there are two distinct coordination environments around the silver atoms of the $Ag_{11}Se$ core unit. Overall, on account of the existence of three alternating triply bridging bromides, the idealized D_{3h} symmetry of the $Ag_{11}Se$ unit observed in Figure 2 is reduced to C_{3h}. Hence, all the dsep ligands are related to each other by the virtual $3/m$ symmetry.

Absorption Spectra and Luminescence Properties. The electronic spectra of the compounds **1**−**3** were measured in dichloromethane solution, and the data are given in Table 3. The spectral profiles of all compounds were quite similar, and each displayed an intense absorption in the 388−392 nm range with a shoulder at 316 nm (Figure 3). The large extinction coefficient of 10^4 indicates a fully allowed transition. The presence of a similar type of absorption band in the identical low-energy region for the $[Ag_{10}(Se)\{Se_2P(OR)_2\}_8]$-type clusters (399 nm)[33] and $[Ag_{11}(\mu_9\text{-Se})(\mu_3\text{-I})_3(Se_2P(OR)_2)_6]$ (398−399 nm)[7] apparently precluded the possibility of considering the bands at 388−392 nm as a

(29) (a) King, R. B. *Inorg. Chem.* **2002**, *41*, 4722–4726. (b) King, R. B. *Inorg. Chim. Acta* **1995**, *228*, 219–224.
(30) Bondi, A. *J. Phys. Chem.* **1964**, *68*, 441–443.
(31) (a) Nayek, H. P.; Massa, W.; Dehnen, S. *Inorg. Chem.* **2010**, *49*, 144–149. (b) Kanatzidis, M. G.; Huang, S.-P. *Angew. Chem., Int. Ed. Engl.* **1989**, *28*, 1513–1514. (c) Zhang, Q.-F.; Cao, R.; Hong, M.-C.; Su, W.-P.; Liu, H.-Q. *Inorg. Chim. Acta* **1998**, *277*, 171–176.
(32) (a) Haiduc, I.; Sowerby, D. B.; Lu, S.-F. *Polyhedron* **1995**, *14*, 3389–3472. (b) Lobana, T.; Wang, J.-C.; Liu, C. W. *Coord. Chem. Rev.* **2007**, *251*, 91–110.
(33) Shang, I.-J. Thesis, Chung Yuan Christian University, Chung-Li, Taiwan, 2000.

Table 3. Photophysical Data for $[Ag_{11}(\mu_9\text{-Se})(\mu_3\text{-Br})_3\{Se_2P(OR)_2\}_6]$ (R = Et, **1**; ^{i}Pr, **2**; ^{2}Bu, **3**)

	state (T/K)	λ_{ex}/nm	λ_{em}/nm[a] (τ_0/ns)	Stokes shift/cm^{-1}	λ_{ab}/nm (ε/dm^3 mol^{-1} cm^{-1})	k_r	k_{nr}	quantum yield[b] Φ_{em}
R = C_2H_5	CH_2Cl_2 (RT)	439	610 (38)	6385	388 (19 637)	4.28×10^4	2.63×10^7	0.0016
	CH_2Cl_2 (77 K)	403	637					
	solid (RT)	441	616 (112)					
	solid (77 K)	379	618					
R = C_3H_7	CH_2Cl_2 (RT)	449	610 (39)	5878	390 (15 845)	4.51×10^4	2.56×10^7	0.0018
	CH_2Cl_2 (77 K)	420	632					
	solid (RT)	391	615 (560)					
	solid (77 K)	379	624					
R = C_4H_9	CH_2Cl_2 (RT)	460	606 (55)	5237	392 (22 702)	3.58×10^4	1.81×10^7	0.002
	CH_2Cl_2 (77 K)	450	623					
	solid (RT)	393	619 (490)					
	solid (77 K)	406	614					

[a] Excited at $\lambda^{ex}_{max.}$. [b] Emission quantum yield measured at 298 K with reference to $Ru(bpy)_3^{2+}$, $\Phi_{em} = 0.06$.

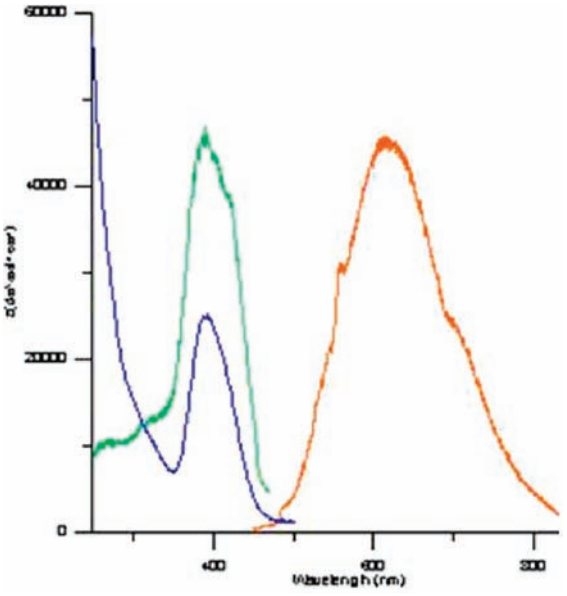

Figure 3. Electronic absorption spectrum (blue), excitation spectrum (green), and emission spectrum (orange) of $Ag_{11}(\mu_9\text{-Se})(\mu_3\text{-Br})_3[Se_2P(O^iPr)_2]_6$ at 298 K.

bromide-to-metal charge transfer transition. The modest red-shift from 388 or 390 to 392 nm for the more electron-rich substituents from ethyl or isopropyl to butyl on the dsep ligands was not sufficient to evaluate the contributions of $Se_2P(OR)_2$. Ligand-centered transitions are shown as the higher energy absorption shoulder at around 300 nm.[7]

Direct excitation of this intense band resulted in a broad emission centered around 610 nm for compounds **1**−**3**. To elucidate the luminescent nature of the systems concerned, we carried out photoluminescent measurements at both 298 and 77 K and found that compounds **1**−**3** exhibited orange luminescence both in solution and in the solid state upon excitation at $\lambda > 379$ nm. The photophysical data and radiative (k_r)/nonradiative (k_{nr}) decay rate constants of the photoexcited state are summarized in Table 3, and spectra at 298 K for cluster **2** are shown in Figure 3. Dichloromethane solutions of clusters were used for measurement of luminescence in solution, and the excitation and emission profiles of all three compounds were very similar. The structureless emission peak of compounds **1**−**3** in the solution featured a maximum at 610, 610, and 606 nm at 298 K, respectively, whereas at 77 K the peak maxima appeared at 637, 632, and 623 nm, that is, shifted ∼20 nm toward the low-energy side of the spectra compared to emission at room temperature. The solid-state photoluminescent spectra of the clusters at both ambient and low temperature were comparable with those in solution. A large Stokes shift (> 5200 cm^{-1}) and the long emission lifetime of **1**−**3** implied the possibility of a large distortion in the excited state and emission from a spin-forbidden triplet emissive state. The lifetime of clusters **1**−**3** was shorter than that observed for their analogous $Ag_{11}(\mu_9\text{-Se})(\mu_3\text{-I})_3[Se_2P(OR)_2]_6$ clusters under identical experimental conditions, possibly due to the intramolecular quenching that occurs within the clusters[34] or the increased radiative rate constant caused by the large spin−orbit coupling and increased nonradiative rate constant due to the high-frequency ligand vibrations.[35] The excitation spectra of the clusters overlap with the low-energy absorption band; hence the emission origin could also be a ligand-to-metal charge transfer with excitation from an orbital associated with the ligand to the metal-based orbital of the excited state. However, the possibility of mixing with a metal-centered (d-s/d-p) silver(I) state cannot be ruled out.

DFT Calculations. In order to achieve a better understanding of the structure and properties of the title compounds and their iodide analogues $Ag_{11}(\mu_9\text{-Se})(\mu_3\text{-I})_3[Se_2P(OR)_2]_6$ (R = ^{i}Pr, ^{2}Bu),[7] DFT and TDDFT calculations were carried out on the simplified models $[Ag_{11}(\mu_9\text{-Se})(\mu_3\text{-X})_3\{Se_2P(OH)_2\}_6]$ (X = Br, I). The results reported here were obtained with the PBE1PBE functional (see Experimental Section), assuming the idealized C_{3h} molecular symmetry. The geometry optimization calculations were carried out with different symmetry constraints (including C_1) and different starting geometries, of which the structure of the idealized C_{3h} symmetry was found to be the most stable. Although some of these optimized geometries differ significantly in terms of their Ag−Ag distances, their energies are very close to that of the C_{3h} geometry. This is indicative of the flexibility of the Ag_{11} cluster cage, the edges of which are associated with weak d^{10}−d^{10} bonding. In both bromo and iodo cases, the optimized C_{3h} structure was characterized as a true minimum

(34) Perreault, D.; Drouin, M; Michel, A; Harvey, P. D. *Inorg. Chem.* **1992**, *31*, 3688–3689.
(35) Henary, M.; Zink, I. J. *Inorg. Chem.* **1991**, *30*, 3111–3112.

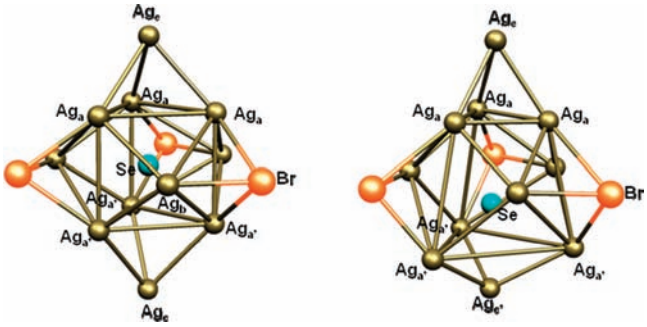

Figure 4. $Ag_{11}(\mu_9\text{-Se})Br_3$ core of the structure of $[Ag_{11}(\mu_9\text{-Se})(\mu_3\text{-Br})_3\{Se_2P(OH)_2\}_6]$ in its C_{3h} singlet ground state (left) and in its C_1 triplet excited state (right). The atom labeling corresponds to that in Table 4.

Table 4. Relevant Computed Data for Models $[Ag_{11}(\mu_9\text{-Se})(\mu_3\text{-X})_3\{Se_2P(OH)_2\}_6]$ (X = Br, I) in Their Ground States ($S = 0$) and in the First Excited Triplet State ($S = 1$) for X = Br[a]

	X = I ($S = 0$) (C_{3h})	X = Br ($S = 0$) (C_{3h})	X = Br ($S = 1$) (C_1)
HOMO−LUMO gap (eV)	3.83	3.88	
Ag_a-Ag_a (Å)	3.755	3.673	2.959 (2.937−2.991)
$Ag_{a'}-Ag_{a'}$ (Å)			4.574 (4.492−4.624)
$Ag_a-Ag_{a'}$ (Å)	3.454	3.516	4.210 (4.111−4.323)
Ag_a-Ag_c (Å)	3.179	3.151	2.960 (2.952−2.974)
			3.023 (3.001−3.035)
Ag_b-Ag_a (Å)	3.265/3.282	3.149/3.458	3.271 (2931−3.888)
Ag_a-X (Å)	3.083	2.984	3.020
$Ag_{a'}-X$ (Å)	3.083	2.984	2.901
Ag_b-X (Å)	2.899	2.787	2.856
$Ag_a-(\mu_9\text{-Se})$ (Å)	2.772	2.755	2.972/3.231
$Ag_b-(\mu_9\text{-Se})$ (Å)	3.134	3.170	2.878
$Ag_c-(\mu_9\text{-Se})$ (Å)	4.052	4.089	5.159(Ag_c)/ 2.834 ($Ag_{c'}$)
$Ag_a-(\mu_2\text{-Se})$ (av; Å)	2.741	2.740	2.733
$Ag_b-(\mu_2\text{-Se})$ (Å)	2.685	2.669	2.704
$Ag_c-(\mu_2\text{-Se})$ (Å)	2.661	2.669	2.743

[a] In the latter case, the inter-atomic distances are averaged and values in parentheses indicate the dispersion range.

on the potential energy surface. Their $Ag_{11}(\mu_9\text{-Se})$ core (Figure 4) was found to be close to D_{3h} symmetry. Given the flexibility of the Ag_{11} cage, the computed metrical parameters (Table 4) are consistent with the corresponding X-ray data of compound **2** and of its iodide analogue.[7] Not surprisingly, both iodide and bromide computed models exhibit very similar electronic structures, and only that corresponding to X = Br is discussed below. Its frontier MO diagram is shown in Figure 5. As expected for a d^{10} metal compound, it has a large HOMO/LUMO gap of 3.88 eV. The HOMO (3e′) is largely delocalized over the whole molecule, while the HOMO−1 (3e″) has a dominant diselenophosphate character. The HOMO−2 (2a″) is also dominated by its diselenophosphate character, but also has significant μ_9-Se and Ag_{11} contributions. Whereas all the other lowest vacant orbitals have a large diselenophosphate character with some silver antibonding admixture, the LUMO can be roughly described

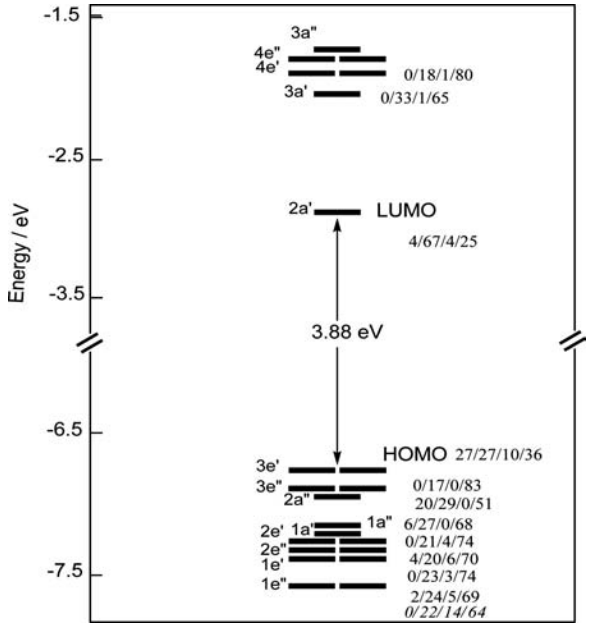

Figure 5. MO diagram of $[Ag_{11}(\mu_9\text{-Se})(\mu_3\text{-Br})_3\{Se_2P(OH)_2\}_6]$ of C_{3h} symmetry. The numerical values indicate the MO localization (in %) on the fragments μ_9-Se/Ag_{11}/Br_3/$[Se_2P(OH)_2]_6$, respectively.

as being the fully bonding combination of σ-type 5s/5p hybrids of 11 Ag atoms. In compact clusters made of nd^{10} metal atoms, such a low-lying vacant in-phase combination of large $(n+1)$s character with some $(n+1)p_\sigma$ admixture is expected.

The bonding mode of the encapsulated selenide can easily be understood on the basis of the electron-accepting ability of the empty cage $[Ag_{11}(\mu_3\text{-X})_3\{Se_2P(OH)_2\}_6]^{2+}$, in which all the Ag atoms are tricoordinated (*vide supra*). The two Ag_c atoms lie in an almost planar coordination and therefore have a low-lying vacant $5p_\sigma$ orbital aligned with the molecular C_3 axis. The nine atoms of the Ag_a and Ag_b types are pyramidally tricoordinated, and their accepting orbital is a 5s/5p σ-type orbital pointing toward the center of the cage. In the C_{3h} molecular symmetry, these 11 σ-type orbitals combine to give 3a′ + 2a″ + 2e′ + 1e″ accepting MOs, of which the lowest, i.e., the most bonding combinations, are of a′, a″, and e′ symmetry. In $[Ag_{11}(\mu_9\text{-Se})(\mu_3\text{-X})_3\{Se_2P(OH)_2\}_6]$, these vacant orbitals interact with the occupied 4s (a′), $4p_z$ (a″), $4p_x$, and $4p_y$ (e′) AOs of the encapsulated selenide to provide strong bonding with the nine atoms of the Ag_a and Ag_b type. The NBO population analysis of Se, $(4s)^{1.82}(4p_z)^{1.84}(4p_{x,y})^{2\times1.84}$ (X = Br) and $(4s)^{1.82}(4p_z)^{1.84}(4p_{x,y})^{2\times1.85}$ (X = I), indicates that the four Se AOs participate equally in the bonding with the empty cages. The corresponding atomic charges of Se (−1.36 and −1.37 for X = Br and I, respectively) and Ag (0.60−0.61 and 0.59−0.61 for X = Br and I, respectively) are consistent with their assigned oxidation states (Se(−II) and Ag(+I)). These results are consistent with previous DFT single-point calculations on related $[Cu_{11}(\mu_9\text{-Se})(\mu_3\text{-I})_3\{Se_2P(OR)_2\}_6]$ compounds.[28]

The optical absorption transitions of the models $[Ag_{11}(\mu_9\text{-Se})(\mu_3\text{-X})_3\{Se_2P(OH)_2\}_6]$ (X = Br, I) were calculated by TDDFT (see Experimental Section). The lowest energy transitions and the corresponding simulated spectra are given in Figure 6. The theoretical results fit the experimental

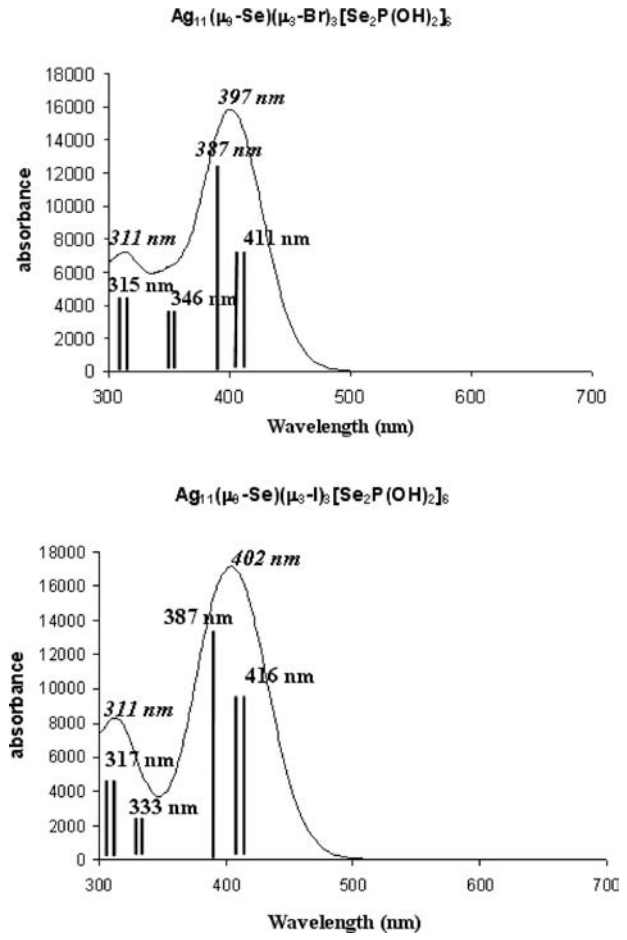

Figure 6. Simulated absorption spectra of $[Ag_{11}(\mu_9\text{-Se})(\mu_3\text{-X})_3\{Se_2P(OH)_2\}_6]$ (X = Br, I). Solid lines represent the calculated electronic transitions, and their lengths are proportional to their oscillator strengths. Values in italics indicate the theoretical λ_{max} values on the simulated curves.

data obtained for compounds **1**−**3** (see above) as well as for their iodide analogues.[7] The band around 400 nm results from two different transitions. That of lower energy corresponds to the doubly degenerate transition HOMO (3e′) → LUMO (2a′). The other one is associated with the HOMO−2 (2a″) → LUMO (2a′) transition. These transitions can be roughly approximated to ligand-to-metal charge transfer. A weak transition at 346 nm (X = Br) and 333 nm (X = I) was computed, which corresponds to the HOMO−5 (2e′) → LUMO (2a′) transition. The next band was computed for both bromide and iodide models at around 311 nm and is mainly associated with a HOMO (3e′) → LUMO+1 (3a′) transition. As far as charge transfer is meaningful in that case, one can say that it occurs between the central Se atom and those on the selenophosphate ligands.

Populating the 2a′ LUMO in the first excited state is expected to induce a significant reduction in the size of the Ag_{11} cluster core, associated with substantial stabilization of 2a′ since this orbital bonds over all the Ag−Ag contacts. Assuming that this effect dominates the emission transition of lowest energy, emission should occur at a lower energy than the corresponding absorption transition. Indeed, this was observed in the spectra of compounds **1**−**3** (*vide supra*). In order to achieve a better understanding of the emission behavior of the title compounds, we computed the emission transition of lowest energy as the energy difference between the first excited triplet state and the singlet ground state. Since the ground state HOMO 3e′ is degenerate, a first-order Jahn−Teller distortion associated with the loss of the C_3 axis was expected in the triplet state. Indeed, the lowest energy for a geometry-optimized triplet state was found for a structure of C_1 symmetry. Surprisingly, this structure can be roughly approximated to C_3, with a small $(Ag_a)_3$ triangle and a large $(Ag_{a'})_3$ triangle (Table 4), the encapsulated Se atom lying closer to the large triangle, in such a way that it is also bound to one of the capping Ag_c atoms, with a corresponding distance of 2.834 Å (Figure 4). Thus, the expected Jahn−Teller distortion is better described as a second-order one, its major component being associated with the loss of the σ_h plane. The major orbitals responsible for this effect are the occupied 2a″ (HOMO−2) and vacant 2a′ (LUMO) MOs. This C_1 structure was computed to be 0.39 eV lower in energy than that optimized under the C_{3h} symmetry constraint. The triplet/singlet energy difference corresponds to a wavelength emission of 526 nm, which is reasonably consistent with the λ_{max} value of the experimental emission band (610 nm). The significant geometrical rearrangement associated with this triplet→singlet emission transition is consistent with the photophysical results (*vide supra*). It is associated with global metal-to-ligand charge transfers.

In conclusion, we have presented here the synthesis and properties of three undecanuclear silver(I) clusters $[Ag_{11}(\mu_9\text{-Se})(\mu_3\text{-Br})_3\{Se_2P(OR)_2\}_6]$ (R = Et, ^{i}Pr, ^{2}Bu), with diselenophoshate ligands that bridge the metal centers in a tetrametallic tetraconnective (μ_2, μ_2) coordination pattern. The clusters have a tricapped trigonal-prismatic geometry. The Ag_{11} core unit with an encapsulated nonacoordinated Se atom is further stabilized by three bromides and six dsep ligands. All three compounds exhibit luminescence both in the solid state and in solution at ambient as well as at low temperatures. Rationalization of the bonding and optical properties of the three compounds is provided through theoretical calculations based on the $[Ag_{11}(\mu_9\text{-Se})(\mu_3\text{-X})_3\{Se_2P(OH)_2\}_6]$ (X = Br, I) models. The computed metrical parameters of the clusters are sufficiently consistent with the corresponding X-ray data of the title compounds. The theoretical calculations confirmed that the low-energy absorptions as well as emissions were ligand-to-metal charge transfer transitions, and a significant structural distortion associated with the loss of the σ_h was revealed in the first excited triplet state due to the second-order Jahn−Teller effect.

Acknowledgment. Financial support from the National Science Council of Taiwan (NSC 98-2911-I-259-002) and from the Institut Universitaire de France (IUF) is gratefully acknowledged. Travel facilities were provided through the French−Taiwanese ORCHID project no. 19667PA.

Supporting Information Available: Crystallographic information for **2** (CIF), ^{1}H, ^{31}P, and ^{77}Se NMR spectra of **1** (Figures S1−S3), and Cartesian coordinates of the optimized models are available free of charge via the Internet at http://pubs.acs.org.